ICSV13 - Vienna
The Thirteenth International Congress on Sound and Vibration
Vienna, Austria, July 2-6, 2006

A MODEL FOR CALCULATING SPECULAR AND DIFFUSE REFLECTIONS IN OUTDOOR SOUND PROPAGATION

Erik M. Salomons*

TNO Science & Industry, PO Box 155, 2600AD Delft, The Netherlands
erik.salomons@tno.nl

Abstract
In many practical outdoor situations, the *direct* sound path between a noise source and a receiver is screened by an obstacle. In these situations *indirect* sound paths become important, in particular *reflections* of sound waves. Reflections may occur at objects such as a vertical wall, but also at the edge of a wood.
In this paper a method is described for the calculation of *i)* specular reflection from a vertical wall and *ii)* diffuse reflection from the edge of a wood. The method is derived from numerical computations and scattering theory, but the resulting formulas are simple enough for implementation in engineering models for outdoor noise.
For a reflection from a vertical wall, the height and width of the wall are taken into account, based on Babinet's principle and results of computations with the Parabolic Equation method for atmospheric sound propagation. The reflection depends on wind and temperature profiles in the atmosphere.
A diffuse reflection from the edge of a wood is modeled as a reflection from a single row of trees, with an effective spacing between the trees that represents the reflection contribution of trees behind this row. The reflection is calculated by incoherent summation of the reflected fields of all the trees in the single row. The calculation of the reflected field of a single tree is based on the theory of scattering of spherical waves by a cylinder. The model takes into account the height, the average diameter, and the spacing of the trees in the wood.

1. SET-UP OF THE MODEL

1.1 Reflection from a Wall

A specular reflection from a wall is modeled by means of an image source (see Fig. 1). The horizontal distance from the image source to the receiver is denoted as R. The sound pressure level of the reflected sound at the receiver is written as

$$L = L_W - A_{geo} - A_{atm} - A_{gr} - A_{refl} \quad (1)$$

where L_W is the sound power level of the source, and the remaining terms are attenuations due to the geometrical divergence of the sound field, atmospheric absorption, the ground effect, and reflection, respectively. We have $A_{geo} = 10\lg 4\pi R^2$ and $A_{atm} = \alpha_{atm} R$, with absorption coefficient α_{atm}. Attenuation A_{gr} is defined as the ground attenuation for propagation from the image source to the receiver (the choice of the atmospheric sound speed profile for this propagation is discussed in Sec. 2). The reflection attenuation is expressed as

$$A_{refl} = -10\lg(\varepsilon_{hor}\varepsilon_{ver}\rho) . \quad (2)$$

Horizontal reflection efficiency ε_{hor} and vertical reflection efficiency ε_{ver} account for the finite width and height of the wall, respectively ($0 \le \varepsilon_{hor} \le 1$, $0 \le \varepsilon_{ver} \le 1$). Reflectivity ρ is a material parameter that accounts for absorption of acoustic energy by the wall ($0 \le \rho \le 1$). For a rigid wall with infinite width and height, we have $\varepsilon_{hor} = \varepsilon_{ver} = \rho = 1$ and $A_{refl} = 0$.

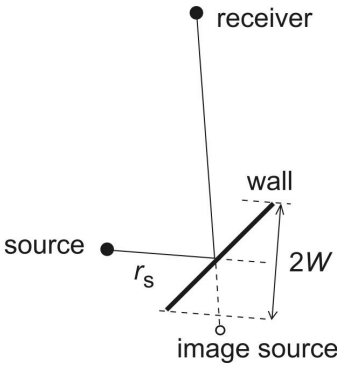

Figure 1. Schematic representation of a reflection by a wall. Indicated are an image source, effective width 2W measured perpendicular to the sound path, and distance r_s from the source to the reflector measured along the sound path.

1.2 Reflection from Trees

Several studies of sound transmission *through* a wood, or forest, have been reported [1,2]. Embleton [3] has presented a model study of sound transmission through a forest, based on the theory of scattering of plane waves by cylinders. Here we present a model for sound *reflection*, based on the theory of scattering of spherical waves by cylinders.

A single tree is modeled as a rigid cylinder. The edge of a wood is modeled as a single row of cylinders with an *effective* spacing between the cylinders. The effective spacing accounts for the contribution to the reflection from trees behind the first row of trees of the wood. This contribution decreases with increasing density of the wood: if the spacing between the trees is small, the reflection from the first row of trees dominates. The value of the effective spacing used in practical calculations should be based on sound measurements.

In the case of reflection from a row of cylinders, all cylinders in the row scatter sound in the direction of the receiver. In other words, a reflection from a row of cylinders is a *diffuse* reflection. We use the single-scattering approximation, so the

total field reflected by the row of cylinders is equal to the sum of the single-scattered fields of the cylinders. Multiple scattering between cylinders is neglected. This is a reasonable approximation for the reflection from the edge of a wood (but not for propagation through a wood).

The scattered fields may be summed coherently, but in practice there is always coherence loss due to atmospheric turbulence. This can be taken into account by a coherence factor [4]. In the limit of strong turbulence, the summation becomes incoherent. From numerical computations we concluded that incoherent summation may be applied for practical calculations.

For computational efficiency, we divide the row of cylinders into a number of segments (see Fig. 2). The energy from segment n is approximated by N_n times the energy from a 'central' cylinder, where N_n is the number of cylinders in the segment. The sound pressure level of the reflected sound is given by the following incoherent sum over the segments:

$$L = 10\lg\left(\sum_n N_n 10^{L_n/10}\right) \tag{3}$$

where

$$L_n = L_{W,n} - A_{geo,n} - A_{atm,n} - A_{gr,n} - A_{refl,n} \tag{4}$$

is the contribution to the sound pressure level from the central cylinder in segment n. The attenuations $A_{geo,n}$, $A_{atm,n}$, and $A_{gr,n}$ are defined as in the previous section. The reflection attenuation is expressed as

$$A_{refl,n} = -10\lg(\varepsilon_{ver}\rho_n) \tag{5}$$

with vertical reflection efficiency ε_{ver} and reflectivity ρ_n ($0 \le \varepsilon_{ver} \le 1$, $0 \le \rho_n \le 1$). Note that the horizontal reflection efficiency is absent in Eq. (5). This is because the reflection is calculated by summing over the row of cylinders. The horizontal size effect is taken into account 'automatically' by this summation.

Vertical reflection efficiency ε_{ver} represents the effect of the finite height of the trees. This is analogous to the effect of the height of a wall on a reflection from the wall. Therefore we use the expression for the vertical reflection efficiency ε_{ver} of a wall reflection also for a reflection from a row of trees. This expression is derived in Sec. 2. For a row of trees, we use the average tree height in this expression instead of the wall height. An expression for reflectivity ρ_n is presented in Sec. 3.

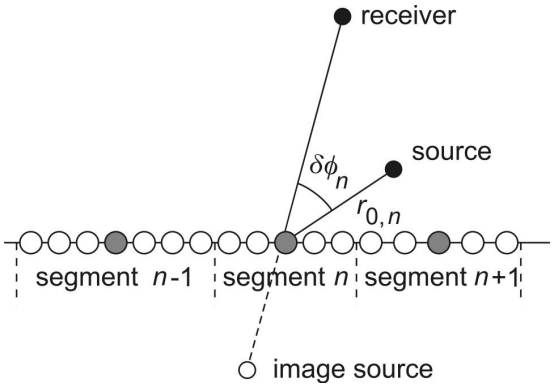

Figure 2. Reflection from a row of cylinders. The row is divided into a number of segments, and each segment is represented by a central cylinder, indicated as a gray circle. An image source is also indicated.

2. REFLECTION EFFICIENCY

2.1 Reflection Efficiency of a Wall in a Non-Refracting Atmosphere

In this section, an expression is presented for the reflection efficiency of a screen, or a wall, in a non-refracting atmosphere. This expression is based on results of numerical computations of sound reflection from a vertical rigid screen with infinite width. The computations were performed with the Parabolic Equation (PE) method [4]. The reflection is taken into account by a Kirchhoff approximation: upon reflection the sound pressure at grid points above the screen is set equal to zero. This approach is analogous to the Kirchhoff approach with PE for diffraction into the shadow region behind a screen [5].

The geometry is shown in Fig. 3. For the PE computations we used the equivalent geometry in Fig. 6. The only difference between Figs. 3 and 6 is that in Fig. 3 the propagation direction is reversed at the reflection while in Fig. 6 it is not reversed. The screen height is denoted as H. The source and the receiver are at distances r_s and r_r from the screen, respectively. The PE computations were performed for a rigid ground surface and a non-refracting atmosphere.

Figure 4 shows PE results of relative sound pressure level $\Delta L = -A_{gr} - A_{refl}$ for six combinations of frequency f and distance r_s, and five heights H. In this case Eq. (2) reduces to $A_{refl} = -10\lg\varepsilon_{ver}$. For large H we have $A_{refl} \to 0$ or $\varepsilon_{ver} \to 1$, and $\Delta L \to -A_{gr}$ (in this case, $-A_{gr} \approx 6\,\text{dB}$). This limiting behavior for large H is observed in Fig. 4. We see further that ΔL decreases with 6 dB by halving H, ΔL decreases with 3 dB by doubling r_s, and ΔL increases with 3 dB by doubling f. Therefore we write

$$\varepsilon_{ver} = \min\left(1, \alpha H^2 / \lambda r_s\right) \quad \text{(for a non-refracting atmosphere)} \tag{6}$$

where λ is the wavelength and α is a constant. To determine constant α, we have plotted in Fig. 5 PE results for A_{refl} versus $-10\lg\varepsilon_{ver}$, with ε_{ver} from Eq. (6). The line represents the best fit, and corresponds with $\alpha = 4.5$. The PE results in Fig. 5 were determined from the results in Fig. 4, for receiver range $r = 1000$ m, using the relations $A_{refl} = -\Delta L - A_{gr}$ and $-A_{gr} \approx 6\,\text{dB}$ (this value of A_{gr} was verified by a PE computation for $H = \infty$).

Equation (6) is valid for $r_r > r_s$. For situations with $r_r < r_s$, reciprocity implies that the expression can be used with r_s replaced by r_r. Equation (6) is valid for a non-refracting atmosphere. The vertical reflection efficiency in a refracting atmosphere is studied in the next section.

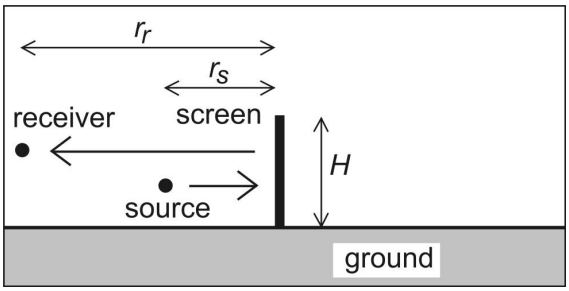

Figure 3. Geometry of reflection from a screen on a ground surface.

Horizontal reflection efficiency ε_{hor} follows directly from Eq. (6) if we use the fact that horizontal gradients in the atmosphere are small, so horizontal refraction can be neglected. From a comparison of Figs. 1 and 3 we see that height H corresponds with width W (the symmetry with respect to the rigid ground surface in Fig. 3 implies that the effective screen dimension is $2H$). This gives

$$\varepsilon_{hor} = \min\left(1, \alpha W^2 / \lambda r_s\right). \tag{7}$$

2.2 Reflection Efficiency of a Wall in a Refracting Atmosphere

The vertical reflection efficiency depends on the vertical sound speed profile in the atmosphere. To explain this, we first recall that the geometry in Fig. 3 is equivalent to the geometry in Fig. 6. It follows from Babinet's principle [6] that the sum of the received field in Fig. 6 and the received field in the complementary geometry in Fig. 7 is equal to the received field in the geometry without obstacles in Fig. 8.

We will now derive a relation between the vertical reflection efficiency and the screen attenuation in the geometry in Fig. 7. We write the received sound pressure in the situations in Figs. 6, 7, and 8 as p_a, p_b, and p_c, respectively. We ignore the ground reflection, for simplicity. Babinet's principle gives $p_a + p_b = p_c$. From Eq. (2) with $\varepsilon_{hor} = 1$ and $\rho = 1$ we have $|p_a|^2 = \varepsilon_{ver} |p_c|^2$. We also have $p_b = D\, p_c$, where D is the (complex) spherical-wave diffraction coefficient [4,7]. Here we assume that the receiver is in the sound shadow of the screen. The screen attenuation A_{scr} is related to D by $A_{scr} = -20\lg(|D|)$. From the above expressions we have $p_a = (1-D)\, p_c$. From the approximation $D \approx \mathrm{Re}(D)$, we find

$$\varepsilon_{ver} = (1-D)^2 \approx \left(1 - 10^{-A_{scr}/20}\right)^2. \tag{8}$$

By PE calculations for a non-refracting atmosphere we verified that this relation is a reasonable and practical approximation. In Ref. [8], a simple model for the screen attenuation A_{scr} as a function of the sound speed profile is described. By using Eq. (8), this model can also be applied to calculate the vertical reflection efficiency as a function of the sound speed profile.

The (effective) sound speed includes the wind component in the propagation direction [4]. Consequently, the sound speed profile is different for the two segments of the propagation path in Fig. 1. We adopt a practical approach and use the profile corresponding with the longer of the two segments. For the ground attenuation A_{gr} (see Sec. 1) the same profile is assumed.

3. REFLECTIVITY OF THE EDGE OF A WOOD

In this section, an expression for reflectivity ρ_n in Eq. (5) is presented. The edge of a wood was represented by a row of cylinders in Sec. 1. For the calculation of reflectivity ρ_n, infinitely long cylinders are assumed. The finite height of the trees is accounted for by the vertical reflection efficiency described in the previous section. From the theory of scattering of spherical waves [9-11] we have derived the following expression for reflectivity ρ_n of a cylinder in segment n:

$$\rho_n = \left| \sum_{m=0}^{\infty} \varepsilon_m \cos(m\,\delta\phi_n)(-i)^m H_m^{(1)}(kr_{0,n}) \frac{J_m'(ka)}{H_m^{(1)}{}'(ka)} \right|^2 , \qquad (9)$$

where $\delta\phi_n$ is the scattering angle and $r_{0,n}$ is the distance from the source to the cylinder (see Fig. 2), $k = \omega/c$ is the wave number, a is the radius of the cylinders, and $\varepsilon_0 = 1$, $\varepsilon_m = 2$ for $m \geq 1$. Further, $H_m^{(1)}$ is the Hankel function of the first kind, $H_m^{(1)}{}'$ its derivative, and J_m' the derivative of the Bessel J-function. For numerical calculations, the sum in Eq. (9) can be truncated at $m = 40$. Equation (9) is valid for situations in which the (central) cylinder is closer to the source than to the receiver. Reciprocity may be applied if the cylinder is closer to the receiver than to the source.

Figure 9 shows an example of reflectivity ρ_n given by Eq. (9) as a function of frequency. Figure 10 shows an example of a reflection at 1000 Hz from a 1000 m long row of equidistant, infinitely long cylinders, for four values of cylinder diameter $2a$ (the row of cylinders can be considered as infinitely long). The graph shows the relative sound pressure level ΔL, defined as the level of the reflection minus the level of a reflection from an infinite rigid wall at the position of the cylinders, as a function of distance d between neighboring cylinders (measured between the axes).

The relation between ΔL and d is simple in this case: $\Delta L \approx -10\lg(d/2a)$. This implies that the reflection from an infinite row of trees can be calculated with Eqs. (1) and (2) for a wall, using the expression $\rho = 2a/d$ for the reflectivity. In the limit that all cylinders touch each other, we have $d = 2a$, and $\rho = 1$. In other words, the reflectivity of an infinite, connected row of cylinders is equal to unity. For low frequency ($ka << 1$), Eq. (9) yields a limiting value of the reflectivity for $d = 2a$ that is smaller than unity. This is probably a consequence of the single-scattering approximation, as one expects that a row of connected cylinders acts as a rigid wall also at low frequency. A practical approach is to model the edge of a wood as a wall with reflectivity $\rho = 2a/d$ for all frequencies.

Acknowledgement. This work was supported by the Dutch Ministry of Defence (DRMW).

REFERENCES

[1] M.A. Price, K. Attenborough and N.W. Heap, "Sound attenuation through trees: measurements and models," J. Acoust. Soc. Am. **84**, 1836-1844 (1988).
[2] M. Swaeringen et al, "Survey of research on sound propagation in forests," Proc. 8th Symp. on Long-Range Sound Prop., Pennsylvania State University, 1998, pp. 131-138.
[3] T.F.W. Embleton, "Scattering by an array of cylinders as a function of surface impedance," J. Acoust. Soc. Am. **40**, 667-670 (1966).
[4] E.M. Salomons, *Computational Atmospheric Acoustics* (Kluwer, Dordrecht, 2001).
[5] E.M. Salomons, "Diffraction by a screen in downwind sound propagation: a parabolic-equation approach," J. Acoust. Soc. Am. **95**, 3109-3117 (1994).
[6] E. Skudrzyk, *The Foundations of Acoustics* (Springer, Wien, 1971) pp. 518-519.
[7] A.D. Pierce, *Acoustics. An Introduction to its Physical Principles and Applications* (American Institute of Physics, Woodbury, 1991).

[8] E.M. Salomons, "Noise barriers in a refracting atmosphere," Applied Acoustics **47**, 217-238 (1996).
[9] J.R. Wait, *Electromagnetic radiation from cylindrical structures* (Pergamon, London, 1959) pp. 1-28.
[10] J.J. Bowman, T.B.A. Senior and P.L.E. Uslenghi, *Electromagnetic and acoustic scattering* (North-Holland, Amsterdam, 1969) pp. 92-128.
[11] P.M. Morse and K.U. Ingard, *Theoretical Acoustics* (McGraw-Hill, New York, 1968).

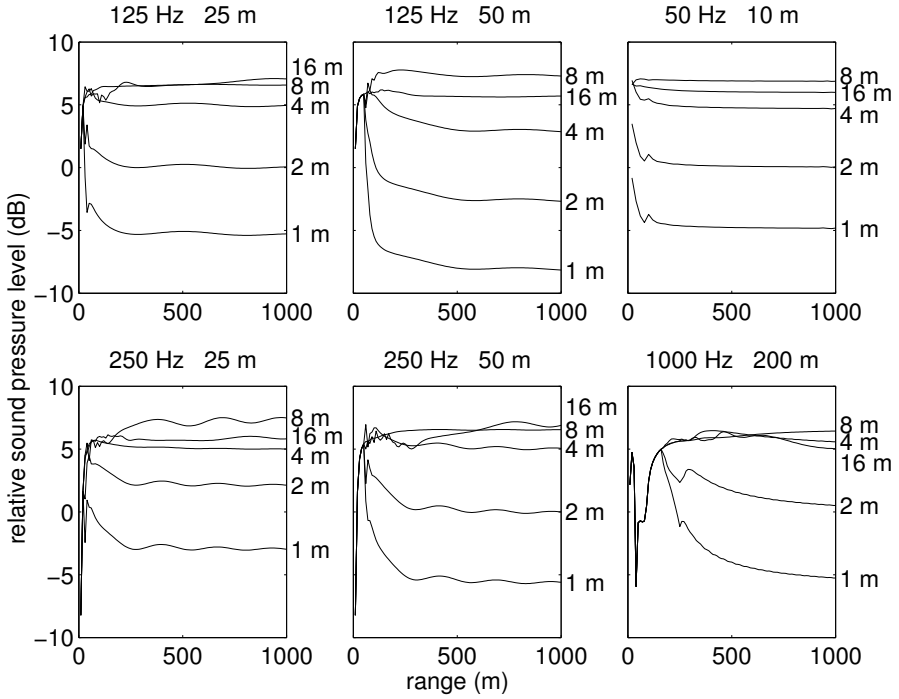

Figure 4. PE results for relative sound pressure level ΔL versus receiver range $r = r_s + r_r$, for six combinations of f and r_s (indicated above the graphs) and five values of H (indicated on the right of the graphs). The results are for a non-refracting atmosphere, a rigid ground, a source height of 2 m and a receiver height of 2 m.

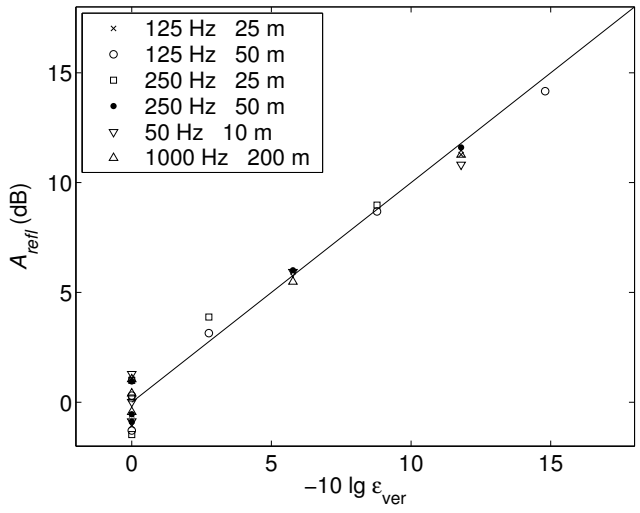

Figure 5. PE results for A_{refl} versus $-10\lg\varepsilon_{ver}$, with ε_{ver} from Eq. (6). The line represents the best fit, and corresponds with $\alpha = 4.5$. The PE results correspond with the results in Fig. 4, for range 1000 m.

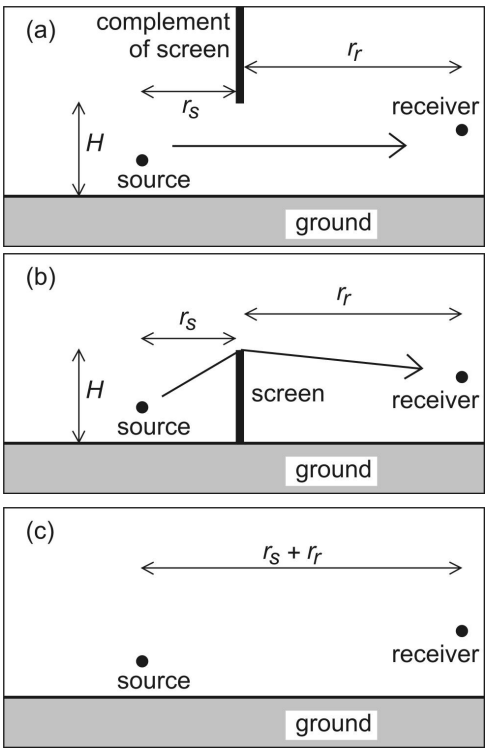

Figure 6. Geometry that is equivalent to the geometry shown in Fig. 3 (in the Kirchhoff approximation).

Figure 7. Complementary geometry of the geometry in Fig. 6.

Figure 8. Geometry similar to the geometry in Figs. 6 and 7, but without obstacles.

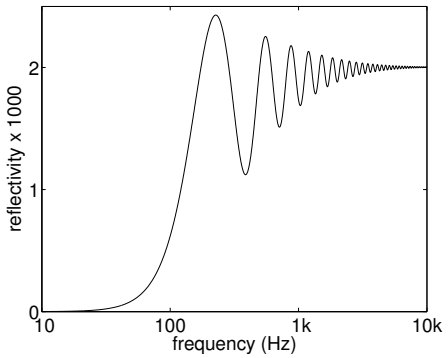

Figure 9. Reflectivity ρ_n given by Eq. (9) as a function of frequency, for a = 0.2 m, $r_{0,n}$ = 50 m and $\delta\phi_n$ = 0.

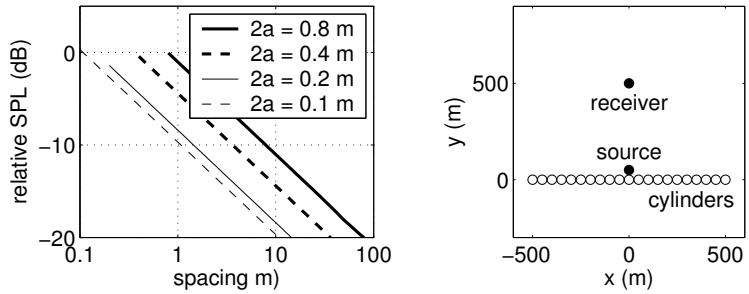

Figure 10. Relative sound pressure level of reflected field at 1000 Hz as a function of the spacing between the cylinders (incoherent summation). A top view of the geometry is shown on the right of the graph.